IJIE Int. J. Indust. Entomol. 36(1) 15-24 (2018)
ISSN 1598-3579, http://dx.doi.org/10.7852/ijie.2018.36.1.15
ISSN 1598-3579 (Print)
ISSN 2586-4785 (Online)

A truncated form of human alpha 1-acid glycoprotein is useful as a molecular tool for insect glycobiology

Daisuke Morokuma[1], Masato Hino[1], Miho Tsuchioka[1], Akitsu Masuda[1], Hiroaki Mon[1], Kazuhito Fujiyama[2], Hiroyuki Kajiura[3], Takahiro Kusakabe[1], and Jae Man Lee[1*]

[1]*Laboratory of Insect Genome Science, Kyushu University Graduate School of Bioresource and Bioenvironmental Sciences, Hakozaki 6-10-1, Higashi-ku, Fukuoka 812-8581, Japan*
[2]*The International Center for Biotechnology, Osaka University, 2-1 Yamada-oka, Osaka 565, Japan*
[3]*Department of Biotechnology, College of Life Sciences, Ritsumeikan University, 1-1-1 Noji-higashi, Kusatsu, Shiga 525-8577, Japan*

Abstract

N-glycosylation is an important posttranslational modification that results in a variety of biological activities, structural stability, and protein-protein interactions. There are still many mysteries in the structure and function of N-glycans, and detailed elucidation is necessary. Baculovirus expression system (BES) is widely used to produce recombinant glycoproteins, but it is not suitable for clinical use due to differences in N-glycan structure between insects and mammals. It is necessary to develop adequate model glycoproteins for analysis to efficiently alter the insect-type N-glycosylation pathway to human type. The previous research shows the recombinant alpha 1-acid glycoprotein (α1AGP) secreted from silkworm cultured cells or larvae is highly glycosylated and expected to be an excellent research candidate for the glycoprotein analysis expressed by BES. Therefore, we improved the α1AGP to be a better model for studying glycosylation. The modified α1AGP (α1AGPΔ) recombinant protein was successfully expressed and purified by using BES, however, the expression level in silkworm cultured cells and larvae were lower than that of the α1AGP. Subsequently, we confirmed the detailed profile of N-glycan on the α1AGPΔ by LS/MS analysis the N-glycan structure at each glycosylation site. These results indicated that the recombinant α1AGPΔ could be usable as a better model glycoprotein of N-glycosylation research in BES.

Int. J. Indust. Entomol. 36(1), 15-24 (2018)

Received : 4 Sep 2017
Revised : 21 Nov 2017
Accepted : 1 Mar 2018

Keywords:
Baculovirus expression system,
N-glycosylation,
Alpha 1 Acid Glycoprotein,
Silkworm

INTRODUCTION

N-glycosylation is one of the major post-translational modifications in eukaryotes and the majority of serum proteins secreted are *N*-glycosylated. Roles and functions of *N*-glycan are highly diverse and are known to be critical in cell-cell communication, adhesion (Takahashi *et al*., 2009), protein structural stability (Öberg *et al*., 2011), and cellular signaling (Boscher *et al*., 2011). Therefore, abnormalities in *N*-glycosylation often result in disease, including developmental deficiency, neurodegenerative disorders or serious tumors (Cazet *et al*., 2010; Pochechueva *et al*., 2012). It is essential

***Corresponding author.**
JaeMan Lee
Laboratory of Insect Genome Science, Kyushu University Graduate School of Bioresource and Bioenvironmental Sciences,
6-10-1 Hakozaki, Fukuoka 812-8581, Japan
Tel. & Fax: +81-92-642-2842
E-mail: jaemanle@agr.kyushu-u.ac.jp

to understand the relationships between the structure and function of *N*-glycans for medical treatment of a particular symptom. Recombinant expression systems of glycoproteins are useful for analyses of their molecular structure, mass-production of antibodies and industrial applications. To this end, the mammalian expression system is often employed for the production of glycoproteins due to its ability to transfer mammalian-type *N*-glycans (Varki, 1993), although it has several disadvantages, such as relatively lower productivity and higher cost.

Baculovirus expression system (BES) using lepidopteran insects or cultured cells has been reported to be suitable for mass-production of xeno-free recombinant proteins with mammalian-like post-translational modifications (Summers, 2006; Kato *et al*., 2010). There are, however, several differences in *N*-glycosylation pathways between mammalians and insects. Glycoproteins secreted from insect cells are paucimannosidic and generally not terminally galactosylated or sialylated (Marchal *et al*., 2001) due to the relatively high activity of b-N-acetylglucosaminidase (FDL) removing the terminal GlcNAc of the hybrid-type structure (Kim *et al*., 2009).

Recently, various studies have been reported to change the *N*-linked glycan structure of insect proteins to terminal sialylated complex type *N*-glycans by transgenic expression of mammalian glycosyltransferases of insect cells (Jarvis, 2003; Harrison and Jarvis, 2006; Toth *et al*., 2014). In these kinds of studies, it is much-need to develop a model glycoprotein to monitor and analyze the *N*-glycosylation linkages easily in insect-BES.

The alpha 1-acid glycoprotein (α1AGP) is derived from human plasma containing five potential *N*-glycosylation sites on the asparagine (Asn) residue in the Asn-X-Ser or Asn-X-Thr tripeptide consensus sequence and is a relatively short peptide of 183 amino acid residues (Fournier *et al*., 2000). In addition, the recombinant α1AGP secreted from silkworm cultured cells or larvae is highly glycosylated and expected to be an excellent research candidate for the glycoprotein analysis expressed by BES (Morokuma *et al*., 2015). However, the *N*-glycosylation sites of α1AGP were concentrated in the half of the amino acid sequence from the N-terminal side (amino acid numbers 1 ~ 85). Therefore, we improved the α1AGP as a model glycoprotein by removing the half part of the amino acid sequence from the C-terminal side and adding the short peptide including two *N*-glycosylation sites at N-terminal. In this study, the recombinant BmNPV expressing the modified α1AGP (α1AGPΔ) containing seven potential *N*-glycosylation sites in truncated short peptide was constructed. We also report the expression, purification, and characterization of the α1AGPΔ secreted from silkworm larvae.

MATERIALS AND METHODS

Cell lines and silkworms

BmN4 cells (a kind gift from Dr. Chisa Aoki), Bme21 cells (Lee *et al*., 2012), BmN4 SID-1 cells (Mon *et al*., 2012), and PS140 cells (a kind gift from Dr. Imanishi, National Institute of Agrobiological Sciences) were maintained in IPL-41 medium (Sigma Chemical) with 10 % fetal bovine serum (GIBCO Invitrogen) at 27°C. The silkworm n17 strain used in this study were supplied by the silkworm stock center in Kyushu University. The larvae were reared on mulberry leaves at 25-27°C.

Recombinant baculovirus

The coding region for human α1AGPΔ was amplified by PCR using the specific primers Hsα1AGPnoSP-5 (5'-CAGATCCCATTGTGTGCCAACCTAG -3') and Hsα1AGPdelta *Xho*I-3 (5'- GTCCCTCGAGCCCACGTATCTGGAGATGG -3'). The PCR product was digested with *Xho*I, and inserted into an *EcoR*V-*Xho*I site of the pENTR11L2130K2NTEVH8 vector. This vector was modified by adding an artificial N-glycosylation site (2N) to pENTR11L2130KTEVH8 vector (Soejima *et al*., 2013). It contains a lobster L21 sequence (for enhancing translation efficiency), signal peptide from silkworm 30kDa protein, and two *N*-glycosylation sites region (5'- GGAGGTA ACGCGACGGGCGGTGGAGGTAACGCGACTGGCGGT -3') at the N-terminal, and the tobacco etch virus (TEV) protease cleavage site for removing the affinity tag from the recombinant protein, the 8-histidine (H8) tag at C-terminal.Baculovirus transfer plasmid was generated by Gateway LR reaction between pDEST8 vector (Invitrogen) and the α1AGPΔ entry plasmid according to the manufacture's protocol. The transfered plasmid (pDEST8-*polh*-30K-α1AGPΔ-TEVH8) was used for the BmNPV baculovirus generation according to the protocols described previously (Ono *et al*., 2007).

Purification of recombinant protein

Approximately 1.0 × 10^5 particles of recombinant virus were injected into 5th instar larvae of n17 silkworm larvae. At 4 dpi, 10 ml of the serum from 25 silkworm larvae was collected into a 15 ml tube containing 20 mM 1-phenyl-2-thiourea, followed by centrifugation at 10,000 *g* for 30 min at 4 ºC. Then the supernatant was transferred into a new tube. The resulting serum was diluted by a binding buffer (20 mM Tris-HCl pH 7.4; 0.5 M NaCl; protease inhibiter tablet (1 tablet /100 ml; Roche); 1 mM PMSF), and centrifuged at 20, 000 *g* for 30 min at 4 ºC. After the filtration through a 0.45-μm filter (Millipore), the supernatant containing recombinant α1AGPΔ was loaded to a nickel affinity chromatography with 5 ml HisTrap excel column (GE Healthcare Bioscience, Piscataway, NJ) and the target protein was eluted by 500 mM imidazole solution buffers.

Endoglycosydase digestions

To cleave *N*-glycan chains, purified the recombinant protein was incubated in 1x Glycoprotein Denaturing Buffer (New England Biolabs) at 95 ºC for 10 minutes. The 20 μL- cleavage reaction contained 2 μL of 10× G7 Reaction Buffer (New England Biolabs), 2 μL of 10% NP40, and 1 μL of Peptide-N-glycosidase F (PNGase F, New England Biolabs). The reaction mixture was incubated at 37°C for 1 hour.

SDS-PAGE and Western blotting

The solution of a1AGPΔ was mixed with the 2x SDS sample buffer (100mM Tris-HCl pH 6.8, 200mM DTT, 4% SDS, 0.02% blomophenol blue, 20% glycerol), denatured at 95°C for 5 minutes and resolved by SDS-PAGE on a 15% gel. Subsequently, proteins in the gels were electrophoretically transferred to PVDF membrane (Millipore) for Western blotting and lectin blotting. For Western blotting, membranes were first blocked for 1 hour in TBST (20 mM Tris-HCl pH 7.5, 500 mM NaCl and 0.1% Tween-20) with 5% skim milk. After incubation, membranes were washed 3 times in TBST for 5 minutes. Thereafter, membranes were incubated with HisProbe-HRP (Pierce) diluted in TBST for 1 hour and washed 5 times in TBST for 5 minutes. After washing, HRP signal was detected with Super Signal West Pico Chemiluminescent Substrate (Pierce) and exposed to medical X-ray film (FUJIFILM). For lectin blotting, the membrane was blocked for 30 minutes with Carbo-Free Blocking solution (Vector Laboratories, USA). Subsequently, the membrane was incubated with ConA (HRP binding, 2 ppm, J-OILMILLS, Japan) diluted for 1 hour with PBST buffer (PBS pH 7.5; 0.05% Tween-20). After washing twice with PBST buffer, the HRP signal was visualized with Super Signal West Pico Chemiluminescent Substrate.

Glycan structural analysis by LC-MS/MS

The purified recombinant glycosylated α1AGPΔ was separated by SDS-PAGE (15 % polyacrylamide gel) and stained by CBB. Bands of interest (Band 1~8) were excised by scalpel, destained with 50 mM NH_4HCO_3 in 50% acetonitrile, dehydrated with acetonitrile, and in-gel digested with trypsin or chymotrypsin in ProteaseMAX™ Surfactant (Promega) at 50˚C for an hour and 25˚C for 12 hours, respectively. The reactions were terminated by the addition of trifluoroacetic acid to a final concentration of 0.1%. The digested peptides were analyzed using nanoLC-MS/MS as previously reported (Kajiura *et al*., 2013). The MS data were analyzed using DataAnalysis 4.0 software (Bruker Daltonics). The ratios of *N*-glycan structures were calculated on the basis of deconvoluted signal intensities of each *N*-glycopeptide.

RESULTS AND DISUCUSSION

Construction of the expression vector

Human a1AGP is composed of 183 amino acid residues without secretory signal peptide, and has five potential *N*-glycosylation sites at Asn-15, -38, -54, -75, and -85. In regard to the secondary structure, human α1AGP contains 25.7 % α-helix, 39.3 % β-strands and 35 % coiled-coil structure, and has two disulfide bonds (connecting Cys residues a.a. 5-147 and a.a. 72-165). Thereby, Human a1AGP forms the β-barrel structure and binds to its various ligands (Schönfeld *et al*., 2008). To increase the ratio of *N*-glycan to total molecular weight, we constructed the mutant of human α1AGP by removing the 90 amino acid residues without N-glycosylation sites from its C-terminus (a.a. 94-183) (Fig. 1A). Therefore, it was predicted

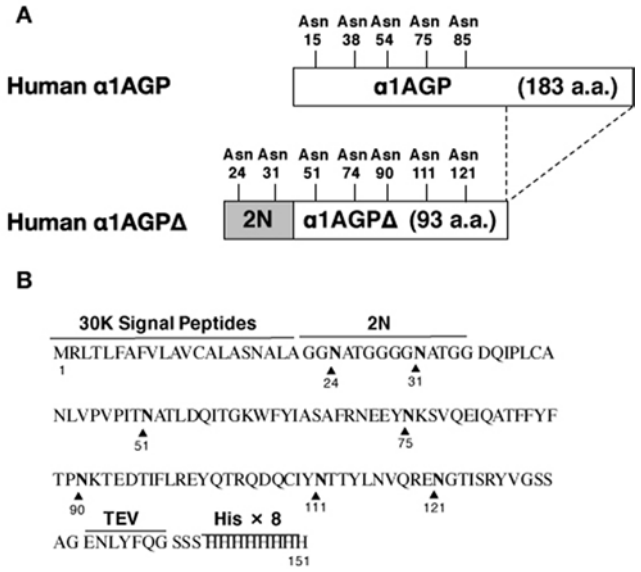

Fig. 1. (A) Schematic representation of the α1AGPΔ in this study. The 90 amino acid sequences were deleted from C-terminus of human α1AGP. Artificial *N*-glycosylation sites (2N) were added N-terminal of 93 amino acid sequences of deleted α1AGP. (B) 151 Amino acid sequences of the recombinant α1AGPΔ. 30K signal peptides and 2N sites were added in N-terminus, and Histidine-tag (His x 8) and TEV protease cleavage site in C-terminus. The asparagine residues (N) to which *N*-glycan may be added indicated by bold letters. The amino acid numbers of asparagine as *N*-glycan sites is shown at the bottom.

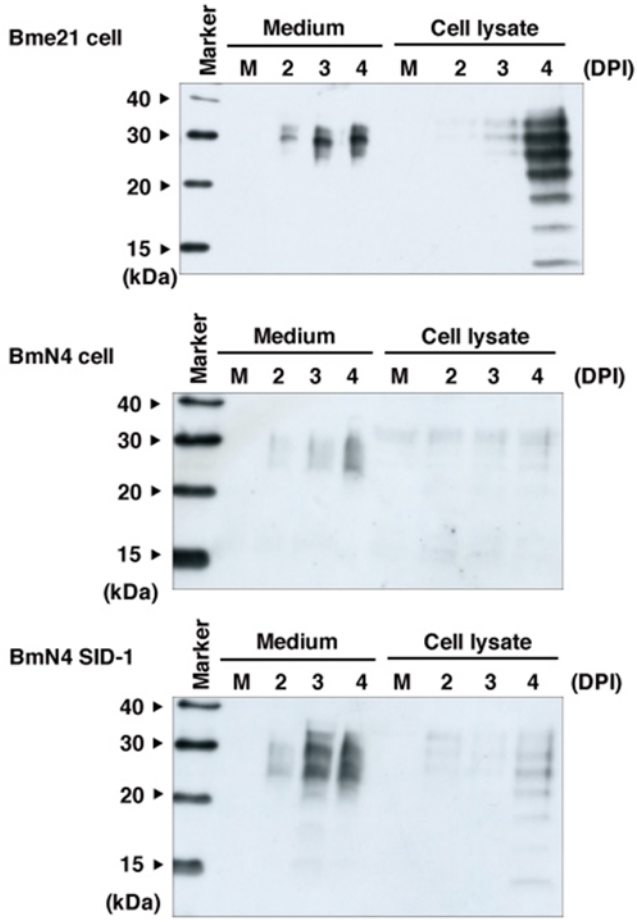

Fig. 2. Expression of the recombinant α1AGPΔ in cultured silkworm cells. Time courses of the expression of the α1AGP protein in Bme21 cells, BmN4 cells and BmN4 SID-1 cells (A). The cells and culture medium were collected at 2, 3, 4 days post-infection (DPI). The recombinant α1AGPΔ was detected by Western blotting using His-Probe.

that the truncation alters its tertiary structure and will cause the loss of ligand binding activities. Besides, 14 amino acid residue containing two *N*-glycosylation sites were added at the N-terminus. As shown in figure 1, the expression construct for the mutant of α1AGP (α1AGPΔ) with the C-terminal His-tag was generated as described under the Materials and Methods. The native signal peptide was replaced with that of silkworm 30K protein to induce effective secretion (Soejima *et al*., 2013). The α1AGPΔ expressed and secreted into silkworm haemolymph is estimated to be 130 amino acid residues with a molecular weight of 14.6 kDa. To evaluate the expression and secretion of α1AGPΔ, the cultured silkworm cells, Bme21, BmN4, and BmN4 SID-1 were infected with the recombinant baculovirus BmNPV/*polh*-30K-α1AGPΔ-TEVH8. As shown in figure 2, the α1AGPΔ was expressed in all cell lines tested and secreted into culture medium. The molecular weight of the α1AGPΔ estimated from the mobility on SDS-PAGE was higher than that it predicted, suggesting that the α1AGPΔ was glycosylated efficiently in silkworm cells.

Purification of α1AGPΔ in Silkworm Larvae

The α1AGPΔ protein from the silkworm haemolymph was purified using nickel affinity chromatography as described under the Materials and Methods. As shown in figure 3A, the purified α1AGPΔ was recovered as plural bands, from 17 kDa to 25 kDa unlike its estimated molecular weight of 15.7 kDa, as well as those from cultured silkworm cells. In addition, the *N*-glycans of purified α1AGPΔ and recombinant α1AGP were able to be cleaved by PNGase F (Figure 3B). Moreover, Western blot using HisProbe-HRP detected the clear seven bands of the α1AGPΔ generated by different *N*-glycosylation. Compared to recombinant human α1AGP, the differences in *N*-glycosylation is more conspicuous in α1AGPΔ using simple SDS-PAGE

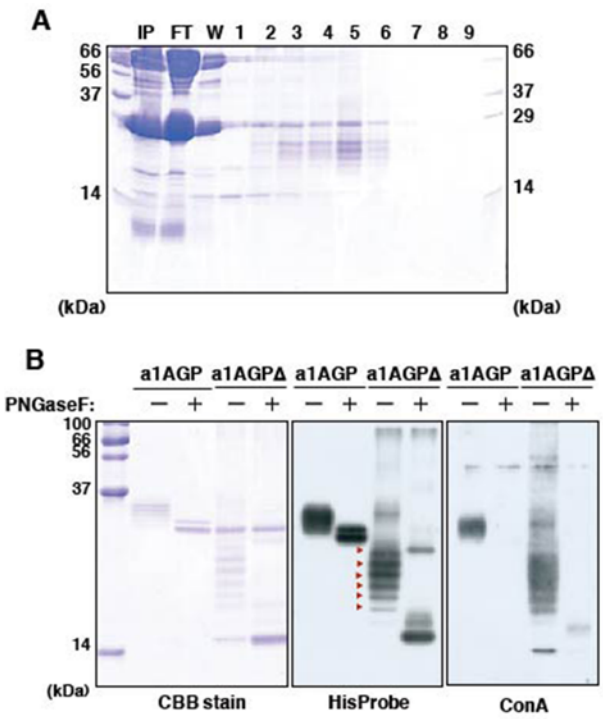

Fig. 3. (A) Purification of human α1AGP from larval haemolymph. The Histidine tagged α1AGPΔ protein was purified through nickel affinity chromatography as described in Materials and methods. Each fraction was resolved on 15% SDS-PAGE and visualized by Coomassie Brilliant Blue (CBB) R-250. IP: input; FT: flow-through fraction; W: wash fraction; Lane No.1~3: eluent fraction (100mM imidazole); Lane No.4~9: eluent fraction (500mM imidazole). (B) Characterization of *N*-glycan structures of the α1AGP secreted in silkworm larval haemolymph. The purified recombinant α1AGP or α1AGPΔ form silkworm larvae as indicated in Materials and methods were incubated with (+) or without (−) PNGaseF for 1 h at 37 °C. After reaction, each mixture was resolved on 15% SDS-PAGE and visualized by CBB R-250, His-Probe, or Concanavalin A (ConA).

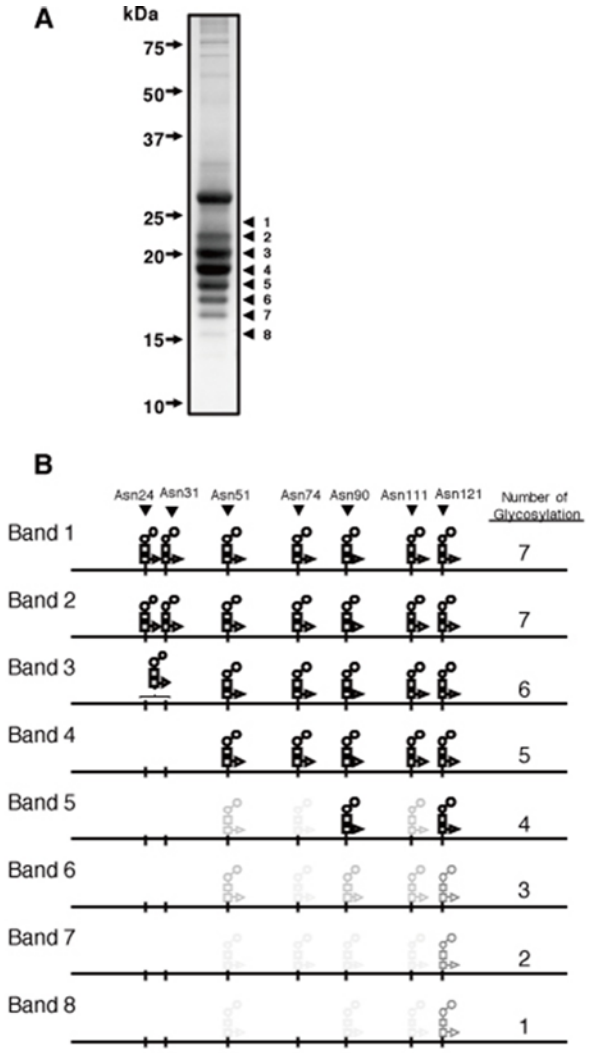

Fig. 4. (A) The purified α1AGPΔ was separated into multiple bands in 15% SDS-PAGE and visualized by CBB R-250. The multiple bands were assigned Band 1 ~ Band 8 from the top. Band 1 is the smear portion at the top of Band 2. (B) The degree of glycosylation of each band 1~ 8 analyzed by LC/MS. At the schematic diagram of *N*-glycan, the open square, open circle and filled triangle represent GlcNAc, mannose and fucose, respectively. The frequency of addition of *N*-glycans at each site is indicated by shading of the diagrams. Approximate number of sugar chains attached to each band is shown on the right.

analysis. Therefore, the α1AGPΔ was expected to become a good model for glycobiological researches such as analysis of the alterations of *N*-glycosylation and elucidating its regulatory mechanisms.

Analyses of the glycan structures of α1AGPΔ

The recombinant α1AGP from silkworm haemolymph is highly glycosylated by paucimannosidic type *N*-glycan (Morokuma *et al*., 2015). In contrast with, the α1AGP from human serum is highly glycosylated by complex-type *N*-glycan (Ceciliani and Pocacqua, 2007), and its carbohydrate structure shows microscopic nonuniformity because of the random formation of biantennary, triantennary, and tetra-antennary complex-type *N*-glycans (Treuheit *et al*., 1992). From figure 4A, the purified α1AGPΔ was visualized by CBB stain and confirmed eight bands (Band 1 ~ 8). We analyzed the number and structure of *N*-glycan on each band of the purified α1AGPΔ by LC/MS analysis. The compositions and relative amounts of the detected *N*-glycans of Band 1~ 8 are shown in Table 1,

Table 1. The ratio of *N*-glycan structure for each sugar chain binding site.

Band 1

Structure			Ratio (%)					
			Asn24, Asn31	Asn51	Ans74	Asn90	Asn111	Asn121
	$HexNAc1$		1.7	-	-	1.0	0.8	0.4
	$DeoxyHex_1HexNAc_1$		2.4	-	-	-	0.3	0.6
	$HexNAc2$		-	-	-	1.3	-	1.0
	$DeoxyHex_1HexNAc_2$		0.7	-	-	-	-	0.9
Mannose type	$Hex_1HexNAc_2$	M1	1.8	-	1.3	0.4	1.1	1.3
	$Hex_2HexNAc_2$	M2	16.1	12.2	12.4	11.6	14.0	10.9
	$Hex_3HexNAc_2$	M3	2.0	12.6	8.3	9.6	6.9	6.7
	$Hex_4HexNAc_2$	M4	-	6.0	1.8	5.6	3.0	2.9
	$Hex_5HexNAc_2$	M5	-	7.7	5.0	10.3	5.4	6.9
	$Hex_6HexNAc_2$	M6	-	-	1.7	4.3	2.5	3.1
	$Hex_7HexNAc_2$	M7	-	-	0.9	2.2	1.8	2.3
	$Hex_8HexNAc_2$	M8	-	-	-	1.6	1.5	2.4
	$Hex_9HexNAc_2$	M9	-	-	-	-	0.7	1.8
	$Hex_{10}HexNAc_2$	GlcM9	-	-	-	-	-	0.6
Fucose-linked	$Hex_1DeoxyHex_1HexNAc_2$	MF	3.9	-	0.9	4.2	0.9	2.4
	$Hex_2DeoxyHex_1HexNAc_2$	M2F	55.1	42.8	50.4	31.2	27.5	44.8
	$Hex_2DeoxyHex_2HexNAc_2$	M2FF	0.9	-	0.8	0.5	0.3	-
	$Hex_3DeoxyHex_1HexNAc_2$	M3F	6.0	18.7	14.9	11.8	6.1	9.9
GlcNAc-linked	$Hex_2HexNAc_3$	GNM2	1.5	-	-	-	0.6	-
	$Hex_3HexNAc_3$	GNM3	-	-	1.7	2.4	2.1	1.2
	$Hex_3DeoxyHex_1HexNAc_3$	GNM3F	-	-	-	1.8	-	-
Total	Mannose type		19.8	38.5	31.4	45.6	36.9	38.8
	Fucose-linked		62.0	61.5	66.9	47.6	34.8	57.1
	GlcNAc-linked		1.5	-	1.7	4.2	2.8	1.2

Band 2

Structure			Ratio (%)					
			Asn24, Asn31	Asn51	Ans74	Asn90	Asn111	Asn121
	$HexNAc1$		1.5	-	-	1.5	1.2	-
	$DeoxyHex_1HexNAc_1$		2.3	-	-	2.3	0.9	-
	$HexNAc2$		0.6	-	-	2.0	-	0.8
	$DeoxyHex_1HexNAc_2$		0.9	-	-	1.1	-	0.7
Mannose type	$Hex_1HexNAc_2$	M1	2.1	0.0	1.3	1.0	1.8	1.3
	$Hex_2HexNAc_2$	M2	21.3	25.0	17.6	19.8	23.1	15.1
	$Hex_3HexNAc_2$	M3	1.3	6.8	3.8	6.4	6.2	3.2
	$Hex_4HexNAc_2$	M4	-	2.8	0.7	2.9	2.1	1.4
	$Hex_5HexNAc_2$	M5	-	3.2	1.3	4.5	3.4	3.2
	$Hex_6HexNAc_2$	M6	-	-	-	1.3	1.5	1.4
	$Hex_7HexNAc_2$	M7	-	-	-	-	1.3	0.8
	$Hex_8HexNAc_2$	M8	-	-	-	-	1.2	0.9
	$Hex_9HexNAc_2$	M9	-	-	-	-	0.5	0.7
	$Hex_{10}HexNAc_2$	GlcM9	-	-	-	-	-	-
Fucose-linked	$Hex_1DeoxyHex_1HexNAc_2$	MF	3.8	-	4.4	5.5	1.4	3.0
	$Hex_2DeoxyHex_1HexNAc_2$	M2F	52.7	55.9	65.9	43.9	47.8	61.6
	$Hex_2DeoxyHex_2HexNAc_2$	M2FF	-	-	-	-	-	-
	$Hex_3DeoxyHex_1HexNAc_2$	M3F	1.4	6.3	4.9	6.0	4.4	5.0
GlcNAc-linked	$Hex_2HexNAc_3$	GNM2	1.3	-	-	-	0.9	-
	$Hex_3HexNAc_3$	GNM3	-	-	-	1.2	1.3	-
	$Hex_3DeoxyHex_1HexNAc_3$	GNM3F	-	-	-	0.8	0.9	0.7
Total	Mannose type		24.6	37.8	24.8	35.8	41.2	28.1
	Fucose-linked		54.1	62.2	75.2	55.3	53.6	69.7
	GlcNAc-linked		1.5	-	-	1.5	3.1	-

respectively. As shown in figure 4B, regarding the number of *N*-glycans, the α1AGPΔ of the Band 1 and Band 2 contain 7 *N*-glycans. Correspondingly, the number of *N*-glycans on the α1AGPΔ of Band 3, Band 4, Band 5, Band 6, Band 7, and Band 8 were 6, 5, 4, 3, 2, and 1, respectively. As shown in Table 1, The LC-MS analysis of PA-glycans from α1AGPΔ by silkworm larvae resulted in the detection of the flowing glycans: $GlcMan_9GlcNAc_2$: GlcM9, $Man_9GlcNAc_2$: M9, $Man_8GlcNAc_2$: M8, $Man_7GlcNAc_2$: M7, $Man_6GlcNAc_2$: M6, $Man_5GlcNAc_2$: M5, $Man_4GlcNAc_2$: M4, $Man_3GlcNAc_2$: M3, $Man_2GlcNAc_2$: M2,

Table 1. Continued

Band 3

Structure			Ratio (%)					
			Asn24, Asn31	Asn51	Ans74	Asn90	Asn111	Asn121
	$HexNAc_1$		1.8	1.1	-	1.6	1.1	-
	$DeoxyHex_1HexNAc_1$		2.2	-	-	2.2	0.8	-
	$HexNAc_2$		0.7	1.3	-	2.2	-	1.1
	$DeoxyHex_1HexNAc_2$		0.8	1.1	1.2	1.1	-	0.8
Mannose type	$Hex_1HexNAc_2$	M1	2.5	2.4	1.5	5.1	1.9	1.1
	$Hex_2HexNAc_2$	M2	25.0	27.4	21.4	25.0	27.0	15.9
	$Hex_3HexNAc_2$	M3	0.9	5.0	2.4	4.3	4.9	2.9
	$Hex_4HexNAc_2$	M4	-	0.6	-	1.6	1.2	1.0
	$Hex_5HexNAc_2$	M5	-	-	-	2.4	1.5	2.1
	$Hex_6HexNAc_2$	M6	-	-	-	0.9	0.6	1.0
	$Hex_7HexNAc_2$	M7	-	-	-	-	-	0.7
	$Hex_8HexNAc_2$	M8	-	-	-	-	-	0.8
	$Hex_9HexNAc_2$	M9	-	-	-	-	-	0.7
	$Hex_{10}HexNAc_2$	GlcM9	-	-	-	-	-	-
Fucose-linked	$Hex_1DeoxyHex_1HexNAc_2$	MF	3.5	-	4.1	2.4	1.7	2.7
	$Hex_2DeoxyHex_1HexNAc_2$	M2F	47.8	54.1	67.3	46.2	55.2	65.8
	$Hex_2DeoxyHex_2HexNAc_2$	M2FF	-	-	-	-	-	-
	$Hex_3DeoxyHex_1HexNAc_2$	M3F	-	3.7	2.2	4.1	2.8	3.4
GlcNAc-linked	$Hex_2HexNAc_3$	GNM2	1.0	-	-	-	0.6	-
	$Hex_3HexNAc_3$	GNM3	-	-	-	0.6	0.7	-
	$Hex_3DeoxyHex_1HexNAc_3$	GNM3F	-	-	-	0.4	-	-
Total	Mannose type		28.4	35.3	25.2	39.3	37.0	26.2
	Fucose-linked		47.8	57.9	73.6	52.6	59.7	71.9
	GlcNAc-linked		1.0	-	-	1.0	1.4	-

Band 4

Structure			Ratio (%)					
			Asn24, Asn31	Asn51	Ans74	Asn90	Asn111	Asn121
	$HexNAc_1$		-	-	-	-	1.2	-
	$DeoxyHex_1HexNAc_1$		-	-	-	-	0.9	-
	$HexNAc_2$		-	1.2	-	2.2	-	1.1
	$DeoxyHex_1HexNAc_2$		-	1.8	-	1.3	-	0.8
Mannose type	$Hex_1HexNAc_2$	M1	-	2.7	2.1	5.5	2.1	1.1
	$Hex_2HexNAc_2$	M2	-	26.6	21.7	26.8	28.8	16.2
	$Hex_3HexNAc_2$	M3	-	5.1	2.4	3.2	3.6	2.0
	$Hex_4HexNAc_2$	M4	-	1.0	-	0.9	-	-
	$Hex_5HexNAc_2$	M5	-	2.1	-	0.9	0.6	1.1
	$Hex_6HexNAc_2$	M6	-	-	-	-	-	-
	$Hex_7HexNAc_2$	M7	-	-	-	-	-	-
	$Hex_8HexNAc_2$	M8	-	-	-	-	-	-
	$Hex_9HexNAc_2$	M9	-	-	-	-	-	-
	$Hex_{10}HexNAc_2$	GlcM9	-	-	-	-	-	-
Fucose-linked	$Hex_1DeoxyHex_1HexNAc_2$	MF	-	3.6	4.2	1.6	1.9	2.7
	$Hex_2DeoxyHex_1HexNAc_2$	M2F	-	53.3	65.1	55.3	58.9	73.0
	$Hex_2DeoxyHex_2HexNAc_2$	M2FF	-	-	2.3	-	-	-
	$Hex_3DeoxyHex_1HexNAc_2$	M3F	-	2.7	2.3	2.3	1.3	1.9
GlcNAc-linked	$Hex_2HexNAc_3$	GNM2	-	-	-	-	0.7	-
	$Hex_3HexNAc_3$	GNM3	-	-	-	-	-	-
	$Hex_3DeoxyHex_1HexNAc_3$	GNM3F	-	-	-	-	-	-
Total	Mannose type		-	37.4	26.2	37.3	35.0	20.5
	Fucose-linked		-	59.6	73.8	59.2	62.1	77.7
	GlcNAc-linked		-	-	-	0.0	0.7	-

$ManGlcNAc_2$: M1, $ManFucGlcNAc_2$: MF, $Man_2FucGlcNAc_2$: M2F, $Man_2Fuc_2GlcNAc_2$: M2FF, $Man_3FucGlcNAc_2$: M3F, $GlcNAcMan_2GlcNAc_2$: GNM2, $GlcNAcMan_3GlcNAc_2$: GNM3, $GlcNAcMan_3FucGlcNAc_2$: GNM3F. Especially, we analyzed the *N*-glycan structure profiles of the α1AGPΔ and confirmed α1AGPΔ is modified by 1 ~ 7 *N*-glycans. Many of them are core-fucosylated pauci-mannosidic type glycans. On the other hand, we comfirmed relatively advanced *N*-glycans in a small proportion. In addition, the *N*-glycosylation numbers of Band 1 and Band 2 are the same, but since the sugar chain structure

Table 1. Continued

Band 5

Structure			Ratio (%)					
			Asn24, Asn31	Asn51	Ans74	Asn90	Asn111	Asn121
	$HexNAc1$		-	-	-	1.5	1.2	-
	$DeoxyHex_1HexNAc_1$		-	-	-	2.7	1.0	-
	HexNAc2		-	-	1.0	2.2	-	1.2
	$DeoxyHex_1HexNAc_2$		-	-	1.7	1.3	-	0.9
Mannose type	$Hex_1HexNAc_2$	M1	-	3.5	1.4	5.2	2.1	1.1
	$Hex_2HexNAc_2$	M2	-	23.0	19.2	22.6	24.0	13.0
	$Hex_3HexNAc_2$	M3	-	4.5	2.9	2.9	3.6	2.4
	$Hex_4HexNAc_2$	M4	-	1.2	-	1.0	-	0.8
	$Hex_5HexNAc_2$	M5	-	-	-	0.9	-	1.4
	$Hex_6HexNAc_2$	M6	-	-	-	-	-	-
	$Hex_7HexNAc_2$	M7	-	-	-	-	-	-
	$Hex_8HexNAc_2$	M8	-	-	-	-	-	-
	$Hex_9HexNAc_2$	M9	-	-	-	-	-	-
	$Hex_{10}HexNAc_2$	GlcM9	-	-	-	-	-	-
Fucose-linked	$Hex_1DeoxyHex_1HexNAc_2$	MF	-	3.7	5.0	6.2	2.0	3.1
	$Hex_2DeoxyHex_1HexNAc_2$	M2F	-	60.2	66.7	51.4	64.1	73.9
	$Hex_2DeoxyHex_2HexNAc_2$	M2FF	-	0.9	-	-	-	-
	$Hex_3DeoxyHex_1HexNAc_2$	M3F	-	3.0	2.2	2.0	1.0	2.2
GlcNAc-linked	$Hex_2HexNAc_3$	GNM2	-	-	-	-	1.0	-
	$Hex_3HexNAc_3$	GNM3	-	-	-	-	-	-
	$Hex_3DeoxyHex_1HexNAc_3$	GNM3F	-	-	-	-	-	-
Total	Mannose type		-	32.2	23.5	32.7	29.7	18.6
	Fucose-linked		-	67.8	73.9	59.5	67.1	79.2
	GlcNAc-linked		-	-	-	-	1.2	-

Band 6

Structure			Ratio (%)					
			Asn24, Asn31	Asn51	Ans74	Asn90	Asn111	Asn121
	$HexNAc1$		-	-	-	1.3	1.3	-
	$DeoxyHex_1HexNAc_1$		-	-	-	3.0	1.2	0.8
	HexNAc2		-	1.9	-	1.9	-	1.3
	$DeoxyHex_1HexNAc_2$		-	3.6	-	1.6	-	1.0
Mannose type	$Hex_1HexNAc_2$	M1	-	10.3	-	4.4	2.1	1.2
	$Hex_2HexNAc_2$	M2	-	18.0	17.7	18.7	20.9	10.5
	$Hex_3HexNAc_2$	M3	-	6.2	3.2	2.9	3.9	2.2
	$Hex_4HexNAc_2$	M4	-	1.4	-	-	-	-
	$Hex_5HexNAc_2$	M5	-	-	-	-	-	-
	$Hex_6HexNAc_2$	M6	-	-	-	-	-	-
	$Hex_7HexNAc_2$	M7	-	-	-	-	-	-
	$Hex_8HexNAc_2$	M8	-	-	-	-	-	-
	$Hex_9HexNAc_2$	M9	-	-	-	-	-	-
	$Hex_{10}HexNAc_2$	GlcM9	-	-	-	-	-	-
Fucose-linked	$Hex_1DeoxyHex_1HexNAc_2$	MF	-	2.0	5.4	7.3	2.4	3.4
	$Hex_2DeoxyHex_1HexNAc_2$	M2F	-	54.5	73.7	57.3	66.1	77.9
	$Hex_2DeoxyHex_2HexNAc_2$	M2FF	-	-	-	-	-	-
	$Hex_3DeoxyHex_1HexNAc_2$	M3F	-	2.1	-	1.5	1.3	1.8
GlcNAc-linked	$Hex_2HexNAc_3$	GNM2	-	-	-	-	0.8	-
	$Hex_3HexNAc_3$	GNM3	-	-	-	-	-	-
	$Hex_3DeoxyHex_1HexNAc_3$	GNM3F	-	-	-	-	-	-
Total	Mannose type		-	35.9	20.9	26.0	26.9	13.9
	Fucose-linked		-	58.6	79.1	66.1	69.8	83.1
	GlcNAc-linked		-	-	-	-	0.8	-

is different from Table 1, it seems that the apparent molecular weight also differs.

In this study, as we aimed, we were able to develop the small molecule protein with more *N*-glycosylation sites. However, the expression level of α1AGPΔ in silkworm cultured cells and larvae was lower than that of the α1AGP. This is considered to be due to the secondary structure being affected by deletion at the C-terminal side. By using α1AGPΔ, it can be expected that changes in *N*-glycan structure can be easily and clearly observed by SDS-PAGE.

Table 1. Continued

Band 7

Structure			Ratio (%)					
			Asn24, Asn31	Asn51	Ans74	Asn90	Asn111	Asn121
	$HexNAc1$		-	-	-	-	-	-
	$DeoxyHex_1HexNAc_1$		-	-	-	-	-	0.9
	$HexNAc2$		-	-	-	-	-	1.5
	$DeoxyHex_1HexNAc_2$		-	-	-	-	-	1.1
Mannose type	$Hex_1HexNAc_2$	M1	-	-	--	8.3	1.8	1.4
	$Hex_2HexNAc_2$	M2	-	23.7	21.0	24.8	11.0	9.5
	$Hex_3HexNAc_2$	M3	-	-	-	3.8	4.2	2.5
	$Hex_4HexNAc_2$	M4	-	-	-	-	-	0.9
	$Hex_5HexNAc_2$	M5	-	-	-	-	-	1.4
	$Hex_6HexNAc_2$	M6	-	-	-	-	-	-
	$Hex_7HexNAc_2$	M7	-	-	-	-	-	-
	$Hex_8HexNAc_2$	M8	-	-	-	-	-	-
	$Hex_9HexNAc_2$	M9	-	-	-	-	-	-
	$Hex_{10}HexNAc_2$	GlcM9	-	-	-	-	-	-
Fucose-linked	$Hex_1DeoxyHex_1HexNAc_2$	MF	-	-	-	10.0	2.1	3.9
	$Hex_2DeoxyHex_1HexNAc_2$	M2F	-	76.3	79.0	53.2	63.1	75.0
	$Hex_2DeoxyHex_2HexNAc_2$	M2FF	-	-	-	-	-	-
	$Hex_3DeoxyHex_1HexNAc_2$	M3F	-	-	-	-	1.4	2.0
GlcNAc-linked	$Hex_2HexNAc_3$	GNM2	-	-	-	-	16.5	-
	$Hex_3HexNAc_3$	GNM3	-	-	-	-	-	-
	$Hex_3DeoxyHex_1HexNAc_3$	GNM3F	-	-	-	-	-	-
Total	Mannose type		-	23.7	21.0	36.9	16.9	15.6
	Fucose-linked		-	76.3	79.0	63.1	66.6	80.9
	GlcNAc-linked		-	-	-	-	16.5	-

Band 8

Structure			Ratio (%)					
			Asn24, Asn31	Asn51	Ans74	Asn90	Asn111	Asn121
	$HexNAc1$		-	-	-	-	-	-
	$DeoxyHex_1HexNAc_1$		-	-	-	-	-	1.0
	$HexNAc2$		-	-	-	-	-	1.0
	$DeoxyHex_1HexNAc_2$		-	-	-	-	-	1.1
Mannose type	$Hex_1HexNAc_2$	M1	-	-	-	9.6	1.7	1.4
	$Hex_2HexNAc_2$	M2	-	23.6	-	23.1	26.2	9.6
	$Hex_3HexNAc_2$	M3	-	-	-	5.6	5.9	3.4
	$Hex_4HexNAc_2$	M4	-	-	-	-	-	1.6
	$Hex_5HexNAc_2$	M5	-	-	-	-	-	1.7
	$Hex_6HexNAc_2$	M6	-	-	-	-	-	-
	$Hex_7HexNAc_2$	M7	-	-	-	-	-	-
	$Hex_8HexNAc_2$	M8	-	-	-	-	-	-
	$Hex_9HexNAc_2$	M9	-	-	-	-	-	-
	$Hex_{10}HexNAc_2$	GlcM9	-	-	-	-	-	-
Fucose-linked	$Hex_1DeoxyHex_1HexNAc_2$	MF	-	-	-	9.1	5.4	4.0
	$Hex_2DeoxyHex_1HexNAc_2$	M2F	-	76.4	-	52.5	58.2	72.1
	$Hex_2DeoxyHex_2HexNAc_2$	M2FF	-	-	-	-	-	-
	$Hex_3DeoxyHex_1HexNAc_2$	M3F	-	-	-	-	2.7	3.2
GlcNAc-linked	$Hex_2HexNAc_3$	GNM2	-	-	-	-	-	-
	$Hex_3HexNAc_3$	GNM3	-	-	-	-	-	-
	$Hex_3DeoxyHex_1HexNAc_3$	GNM3F	-	-	-	-	-	-
Total	Mannose type		-	23.6	-	38.3	33.8	17.7
	Fucose-linked		-	76.4	-	61.7	66.2	79.3
	GlcNAc-linked		-	-	-	-	-	-

ACKNOWLEDGEMENT

This work was supported in part by a grant KAKENHI No. 15H04612 from the Japan Society for the Promotion of Science. The authors declare no conflict of interest.

REFERENCES

Boscher C, Dennis JW, Nabi, IR (2011) Glycosylation, galectins and cellular signaling. Curr Opin Cell Biol 23(4), 383-92.

Cazet A, Julien S, Bobowski M, Burchell J, Delannoy P (2010) Tumour-

associated carbohydrate antigens in breast cancer. Breast Cancer Res 12, 204.

Ceciliani F, Pocacqua V (2007) The acute phase protein alpha1-acid glycoprotein: a model for altered glycosylation during diseases. Curr Protein Pept Sci 8, 91-108.

Fournier T, Medjoubi-NN, Porquet D (2000) Alpha-1-acid glycoprotein. Biochim Biophys Acta 1482, 157-71.

Harrison RL, Jarvis DL (2006) Protein *N*-glycosylation in the baculovirus-insect cell expression system and engineering of insect cells to produce "mammalianized" recombinant glycoproteins. Adv Virus Res 68, 159-191.

Jarvis DL (2003) Developing baculovirus-insect cell expression systems for humanized recombinant glycoprotein production. Virology 310, 1-7.

Kajiura H, Wasai M, Kasahara S, Takaiwa F, Fujiyama K (2013) *N*-glycosylation and *N*-glycan moieties of CTB expressed in rice seeds. Mol Biotechnol 54, 784-794.

Kato T, Kajikawa M, Maenaka K, Park EY (2010) Silkworm expression system as a platform technology in life science. Appl Microbiol Biotechnol 85, 459-470.

Kim YK, Kim KR, Kang DG, Jang SY, Kim YH, Cha HJ (2009) Suppression of b-Nacetylglucosaminidase in *N*-glycosylation pathway for complex glycoprotein formation in Drosophila S2 cells. Glycobiology 19, 301-308.

Lee JM, Kawakami N, Mon H, Mitsunobu H, Iiyama K, Ninaki S, *et al.* (2012) Establishment of a Bombyx mori nucleopolyhedrovirus (BmNPV) hyper-sensitive cell line from the silkworm e21 strain. Biotechnol Lett 34, 1773-1779.

Marchal I, Jarvis DL, Cacan R, Verbert A (2001) Glycoproteins from insect cells: sialylated or not? Biol Chem 382, 151-159.

Mon H, Kobayashi I, Ohkubo S, Tomita S, Lee JM, Sezutsu H, *et al.* (2012) Effective RNA interference in cultured silkworm cells mediated by overexpression of *Caenorhabditis elegans* SID-1. RNA Biol 9, 40-46.

Morokuma D, Xu J, Mon H, Hirata K, Hino M, Kuboe S, *et al.* (2015) Human alpha 1-acid glycoprotein as a model protein for glycoanalysis in baculovirus expression vector system. J Asia Pac Entomol 18(2), 303-309.

Öberg F, Sjöhamn J, Fischer G, Moberg A, Pedersen A, Neutze R, *et al.* (2011) Glycosylation increases the thermostability of human aquaporin 10 protein. J Bio Chem 286(36), 31915-23.

Ono C, Nakatsukasa T, Nishijima Y, Asano S, Sahara K, Bando H (2007) Construction of the BmNPV T3 bacmid system and its application to the functional analysis of BmNPV he65. J Insect Biotech Sericol 76, 161-167.

Pochechueva T, Jacob F, Fedier A, Heinzelmann-schwarz V (2012) Tumor-associated glycans and their role in gynecological cancers: accelerating translational research by novel high-throughput approaches. Metabolites 2(4), 913-39.

Schönfeld DL, Ravelli RB, Mueller U, Skerra A (2008) The 1. 8-Å crystal structure of α 1 -acid glycoprotein (Orosomucoid) solved by UV RIP reveals the broad drug-binding activity of this human plasma lipocalin. J Mol Biol 384(2), 393-405.

Soejima Y, Lee JM, Nagata Y, Mon H, Iiyama K, Kitano H, *et al.* (2013) Comparison of signal peptides for efficient protein secretion in the baculovirus-silkworm system. Cent Euro J Biol 8(1), 1-7.

Summers MD (2006) Milestones leading to the genetic engineering of baculoviruses as expression vector systems and viral pesticides. Adv Virus Res 68, 3-73.

Takahashi M, Kuroki Y, Ohtsubo K, Taniguchi N (2009) Core fucose and bisecting GlcNAc, the direct modifiers of the *N*-glycan core: their functions and target proteins. Carbohydr Res 344(12), 1387-1390.

Toth AM, Kuo CW, Khoo KH, Jarvis DL (2014) A new insect cell glycoengineering approach provides baculovirus-inducible glycogene expression and increases human-type glycosylation efficiency. J Biotechnol 182–183, 19-29.

Treuheit MJ, Costello CE, Halsall HB (1992) Analysis of the five glycosylation sites of human alpha 1-acid glycoprotein. Biochemical J 283 (Pt 1), 105-112.

Varki A (1993) Biological roles of oligosaccharides: all of the theories are correct. Glycobiology 3(2), 97-130.